Chemical reaction facilitates nanoscale mixing†

Alexander Patashinski,*[ab] Rafal Orlik,[c] Mark Ratner[a] and Bartosz A. Grzybowski*[ab]

Received 27th April 2010, Accepted 21st June 2010
DOI: 10.1039/c0sm00291g

To investigate the nature of mixing in reacting liquids, a two-dimensional system comprising two partly miscible liquids A and B that can form surface-active AB dimers was studied using Molecular Dynamics simulations. In the initial state, A and B occupied different parts of the system and were separated by a planar interface. Due to the A + B ↔ AB reaction, this interface became unstable and the liquids mixed. When the reaction was fast, it facilitated pronounced flows on molecular as well as larger scales. These non-equilibrium motions broke-up large, homogeneous regions into progressively smaller clusters surrounded by the AB dimers. This process substantially enhanced the mixing of A and B. The reaction created a variety of markedly different final morphologies depending on the reaction rate, component miscibility, and other parameters.

1. Introduction

Chemical reactions can take place only when the reacting molecules are brought to within a fraction of a nanometre from one another. To achieve this, reactants have to be mixed to nanometre scales. Molecular diffusion provides means for mixing reacting species, but it is a slow process, especially when the reaction products create a non-permeable "protective" layer around unreacted substrates. Mechanical blending can break-up liquid components into small droplets and can thus create an extended interface for the reaction to commence. Still, the process is limited by the sizes of the droplets (typically, down to few microns) and by diffusion of the reagents through the droplet/solvent interface. Interestingly, even in the absence of mechanical agitation, some reacting species mix much faster than what could be explained by molecular diffusion alone. A widely studied example of extremely fast mixing on very small length-scales is the industrially important reaction of isocyanites and polyols involved in the production of polyurethanes.[1–3] It was suggested[2] that this fast mixing is due to reaction-induced instabilities of the interface between the reacting species, and that these instabilities can break-up micrometre-scale droplets into nanometre-scale "vesicles".

On macroscopic length-scales, interfacial instabilities created by non-equilibrium conditions have been studied both experimentally[4–8] and theoretically.[8–12] Several general mechanisms were suggested[4–12] to explain the observed phenomena. Depending on a specific situation, convection flows due to temperature gradients, gravity-induced flows due to non-uniform density, Marangoni convection, and turbulence have all been considered.[13] Accumulation and self-assembly of reaction products at the interface can also change surface tension, and significant overpopulation of the interface by these products can make the interface unstable. This type of behaviour is seen in "self-dividing" droplets reported in ref. 14–16.

While large-scale instabilities can be studied using continuum approaches of chemical kinetics and hydrodynamics,[8,9,17] understanding reactive mixing at nanometre and sub-nanometre scales requires microscopic theory. Analytical solution of microscopic equations of motion for many reacting molecules is a known challenge even for the simplest systems, so these equations have to be solved numerically.

In this paper, we implement Molecular Dynamics (MD) simulations to explore the concept of reaction-driven nanoscale mixing. Specifically, we study a two-dimensional (2D) model system which initially comprises two phase-separated liquids, A and B (Fig. 1). These liquids can engage in a chemical reaction and can form AB dimers whose self-organization at the liquid–liquid interface(s) influences the effective surface tension, and gives rise to interfacial instabilities on various length-scales. Under non-equilibrium conditions, these instabilities amplify

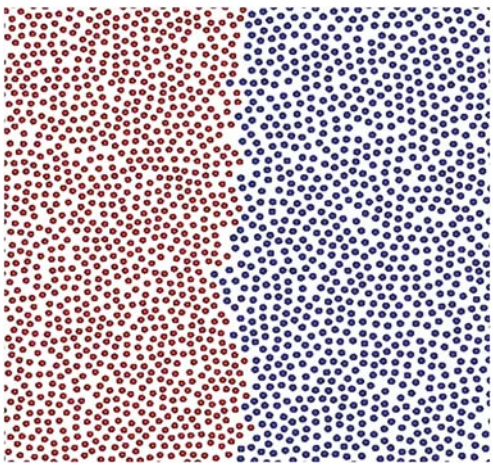

Fig. 1 A typical initial configuration of the system comprising non-reacted A and B particles. The liquids are phase separated and the interface between them is "wrinkled" only due to thermal fluctuations.

[a]*Department of Chemistry, Northwestern University, 2145 Sheridan Road, Evanston, IL, 60208-3113, USA. E-mail: a-patashinski@northwestern.edu; grzybor@northwestern.edu*
[b]*Department of Chemical and Biological Engineering, Northwestern University, 2145 Sheridan Road, Evanston, IL, 60208-3113, USA. E-mail: grzybor@northwestern.edu*
[c]*Orlik Software, ul. Lniana 22/12, 50-520 Wrocław, Poland*

† Electronic supplementary information (ESI) available: Two movies illustrating the mixing process for various values of the K and k parameters. See DOI: 10.1039/c0sm00291g.

into fingering and/or vesicular patterns that increase the interfacial area and effectively enhance reactive mixing.

2. Simulation model

Interactions between A and A and between B and B particles were taken as repulsive at short distances and attractive at larger distances, and were described by the familiar Lennard-Jones potential; the interaction between A and B particles was repulsive:

$$\begin{aligned} U_{AA}(r) &= 4\varepsilon\left[\left(\frac{\sigma_A}{r}\right)^{12}-\left(\frac{\sigma_A}{r}\right)^{6}\right], \quad U_{BB}(r) \\ &= 4\varepsilon\left[\left(\frac{\sigma_B}{r}\right)^{12}-\left(\frac{\sigma_B}{r}\right)^{6}\right], \quad U_{AB}(r) = 4\varepsilon K\left(\frac{\sigma_{AB}}{r}\right)^{12}, \quad \sigma_{AB} \\ &= \frac{\sigma_A+\sigma_B}{2} \end{aligned} \tag{1}$$

Parameter K controlled the strength of the A–B repulsion and, effectively, the miscibility of A and B in the absence of reaction. The units of length, temperature (energy), and mass were all rescaled with respect to the A-particle properties: $\sigma_A = 1$, $\varepsilon = 1$, and $m_A = 1$. The mass of B particles was $m_B = m_A\,(\sigma_B/\sigma)^2$. The units of length, energy, and mass also defined the time unit, $\tau_0 = \sigma(M/\varepsilon)^{1/2}$, which was of the same order of magnitude as the thermal-vibration period τ of A particles. The MD step had the duration $h = 0.0064 \approx 0.002\tau$ (or $\tau \approx 500h$). Rescaling procedures were similar to those used in monocomponent, "pure A" systems without reaction that were studied previously.[18,20]

MD simulations with periodic boundary conditions (see, for example ref. 18) typically lasted for 3.05×10^6 to 6.5×10^6 MD steps (h), and were run according to a modified (NVE) Verlet algorithm accounting for the reaction of A and B into AB dimers. Once bound within a dimer, the interactions of its A and B components with other particles (*i.e.*, with free A, free B, or other dimers) were prescribed by potentials given in eqn (1). The (NVE) algorithm conserves the energy of the system, and thus simulates adiabatic conditions. In our model, the reaction was exothermic, and the temperature of the adiabatic system increased from $T = 3$ at the beginning to $T = 3.5$–5 at the end of a run. We note that simulations using the (NVT) ensemble were also conducted for selected initial conditions. The results of these isothermic runs were qualitatively similar to those in the corresponding (NVE) ensemble although dimer production under (NVT) conditions was predictably slower.

Since the initial configuration comprised crystalline domains, it was first equilibrated by heating-up such that the domains "melted". The equilibrium was controlled by tracking the potential energy and energy fluctuations reaching a stationary level. The equilibration time depended on the temperature; for $T = 3$, this time was $5 \times 10^4 h$ steps. The chemical reaction between A and B was allowed only after the system was initially equilibrated. The reaction was then modelled by replacing, under certain predetermined conditions, the reacting particles A and B by the AB product/dimer. The algorithm of this replacement was prescribed as follows:

(i) At any MD step, if the distance r between non-reacted A and B particles was smaller than some threshold value r_0, a random variable $0 \leq \mathrm{RND} \leq 1$ was generated;

(ii) If $\mathrm{RND} < k$, the binding potential $W(r) = -\beta e^{-\alpha(r-r_D)^2}$ was turned on between these particles. In this way, the parameter k controlled the rate of "reactive collisions" and together with other factors (density, particle sizes, and probability for free A and B to come to within r_0) effectively determined the rate of the reaction. Distance r_D played the role of the "equilibrium" dimer size.

(iii) The A and B particles within a dimer were excluded from further bonding. To prevent thermal break-ups of dimers, a very deep ($\beta = 150$) and narrow ($\alpha = 100$) binding potential was used, and the distance $|r_D - r_0|$ was kept small, $\alpha(r_D - r_0)^2 \ll 1$.[19]

In the absence of reaction, the (NVE)-algorithm conserves the total energy of the system. Creation of dimers generates non-equilibrium conditions: when a dimer is created, the energy of the system instantly changes (diminishes). If the distance between A and B at the time of binding is $r_b \approx r_0$, then the change in potential energy is $W(r_b) < 0$ while the kinetic energy is conserved. If, at time t, there are $N_D(t)$ dimers in the system, the energy-conserving quantity is $F = E - N_D(t)\langle W(r_b)\rangle$, where the brackets denote an average value. Creation of dimers also perturbs the local equilibrium if the potential energy $W(r) + U_{AB}(r)$ for the intra-dimer motions (at the instant of dimer creation) is large compared to the thermal energy of other degrees of freedom. Collisions with surrounding particles result in the equilibration of these motions, so the excess energy is converted to heat. For our choice of parameters, the average per-dimer heat of an exothermic reaction was $\Delta W \approx W(r_0) - W(r_D)$. For simulations starting at the initial temperature $T = 3$, the temperature at the end of the run was $T \approx 4$–5.

The coefficient K in the repulsion potential (last line in (1)) controlled the mutual solubility of the A and B components and of the AB dimers. The same parameter also controlled the activation energy $U_{AB}(r_0) = 4K/r_0^{12}$ for neighbouring A and B particles to reach the reaction distance r_0, and thus it determined the probability $p(r_0) \approx \exp[-U_{AB}(r_0)/T]$ of finding these particles at the reaction distance. The frequency of reactive collisions depended on both $p(r_0)$ and the reaction parameter k. For the range of temperatures and densities studied here, the time for proximal A and B to react was about τ for $k > 0.01$. For $k = 10^{-5}$, the probability of reaction at the first "exposure" of A to B was negligibly small for all thermodynamic conditions.

3. Results and discussion

With the methodology thus defined, we studied how the final morphology of the mixture depends on the miscibility parameter K and on the reaction parameter k in a two-dimensional (2D) system comprising 1250 of A and B particles each. Particles configurations were sampled at time intervals $\Delta t = 10\,000h$. In addition to "still configurations" (*e.g.*, Fig. 2a), images have been combined into "movies" available as part of the ESI†.

General results

The key result of our simulations (summarized in Fig. 2) is that the chemical reaction induces intense mixing at both molecular and larger length-scales. The magnitudes of particles' collective motions are much larger than those observed in the absence of reaction.

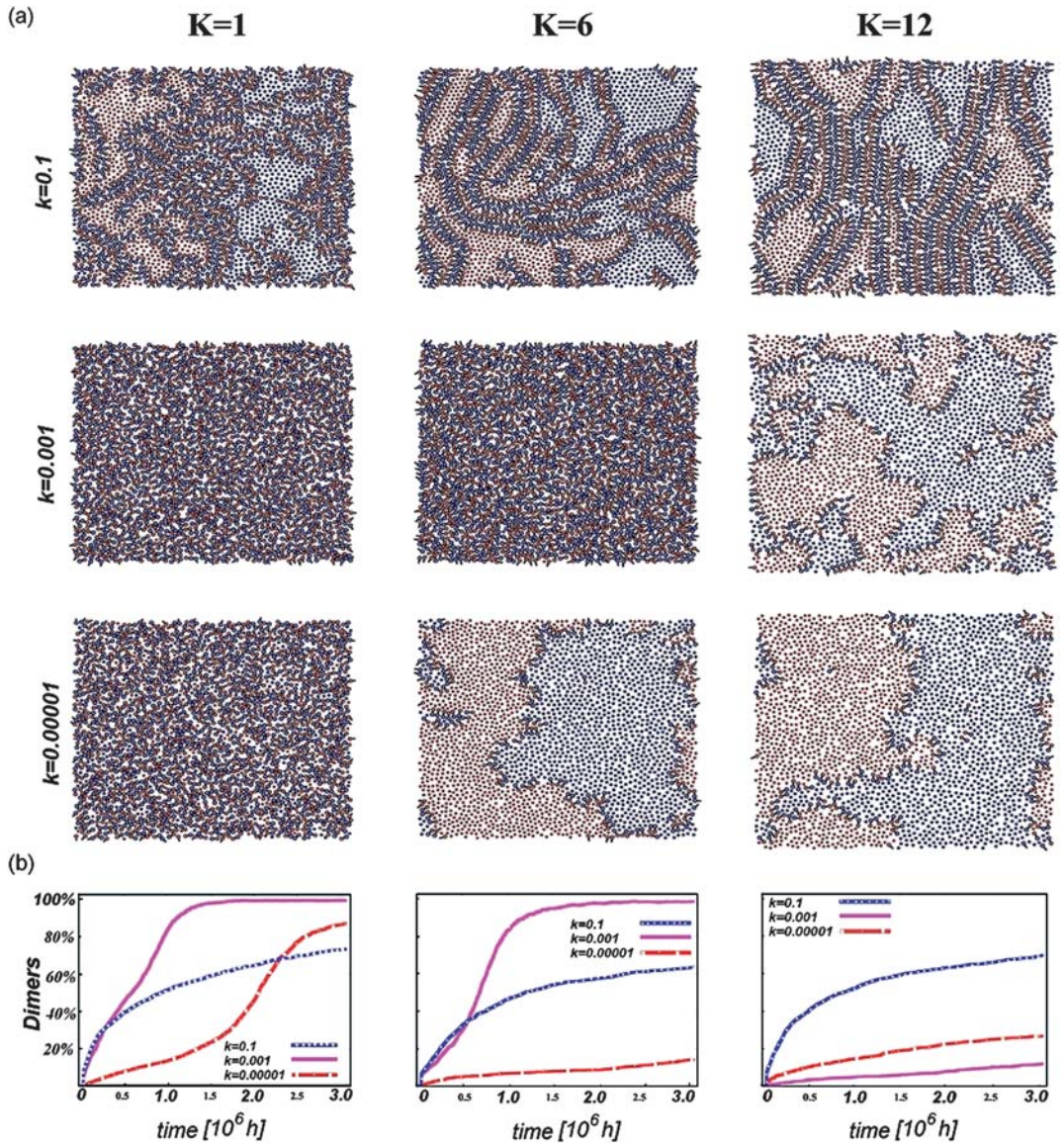

Fig. 2 (a) Final configurations of the system ($t = 3.05 \times 10^6 h$) for different values of controlling parameters k and K as indicated in the pictures. The small k and large K configurations represent, because of slow reaction, configurations far from the completion of the reaction. (b) Graphs plot the production of dimers as a function of time for different values of k and K.

(i) No reaction. Without reaction and dimer formation, diffusion mixing at the time-scale of simulations was slow: even for the largest miscibility at $K = 1$, the average fraction of A-particles surrounded by the B-phase (or B-particles surrounded by the A-particles) was only about 1% at the end of simulation ($t = 3.05 \times 10^6 h$). For lower miscibility (*e.g.*, $K = 6$ or 12) and reaction turned off ($k = 0$), no "dissolved" particles were observed at all. In all cases, the A–B interface remained sharp with exception of small "wrinkles" due to thermal fluctuations. At the molecular scale, these wrinkles can be construed as thermally excited capillary waves with amplitudes determined by effective surface tension, α. In the macroscopic limit, the energy δE to create a wrinkle of a size (length) l and amplitude h is $\delta E \approx h^2/l$. For the thermally excited wrinkles, $\delta E \approx T$ and $h \approx (Tl)^{1/2}$. In our simulations without dimer formation, the amplitudes of the interfacial "wrinkling" decreased when the parameter K (controlling surface tension and miscibility) increased.

(ii) With reaction present. Changing the controlling parameters K and k resulted in large changes in the time-schedules of dimer formation. The final (at the end of the MD runs) morphologies varied from emulsion-like structures to ordered double-layers of dimers (analogous to 2D-lamellar or 3D cylindrical phases). Fig. 2a has a representative set of configurations at $t = 3.05 \times 10^6 h$. In all these simulations, the initial temperature was $T = 3$, and the average distance between particles at $t = 0$ was 1.10. The corresponding time-schedules of dimer production are shown in Fig. 2b. The particular values of $K = 1$, 6, and 12 (in the figure's columns) range from moderately miscible to immiscible fluids; the range $k = 0.1$, 0.001, and 0.00001 includes fast reactions (for $k = 0.1$, proximal A's and B's reacted in

$\tau \approx 500h$) and slow reactions (for $k = 0.00001$, the reaction time for proximal A and B was about 10^6h and most particles were unreacted at the end of the run).

Generally, faster reactions and lower miscibilities (higher surface tension) favour formation of large-scale, ordered double-bands of dimers. In this context, we note that although the absolute minimum of the system's potential energy corresponds to a 2D-lamellar "crystal" featuring parallel bands of dimers (with opposite orientations of these dimers in neighbouring bands), this "perfect" structure was never realized in the simulations because of kinetic limitations. Instead, the relatively low-energy final states featuring micelles or dual-layered filaments of the lamellar structure were observed (see Fig. 2a). These structures originated from the fluctuations/'wrinkling' of the A–B interface. Immediately after the reaction was turned on, interfacial wrinkles had modest amplitudes which, however, grew when the density of dimers at the interface increased. The time of this increase initially depended on the reaction parameter k, but at later times, when the density of interfacial dimers increased, the dynamics and morphology of wrinkles were dictated mostly by the parameter K.

A rather general pattern, observed at different values of k and K, was the appearance of "fingers" and their fluctuation break-up. This pattern can be seen most clearly in the large-K and large-k final configurations in Fig. 2a, but is perhaps best visualized in the movies (ESI†) composed of sampled configurations.

Qualitatively, formation of the "fingers" can be attributed to the surfactant-like organization of the dimers along the interface: when many dimers are produced, the surface tension at the interface becomes small or negative. In the simulations, when about half of the interface is populated by dimers, the interface becomes unstable and prone to significant "wrinkling" fluctuations—some of these wrinkles develop into finger-like structures. Importantly, this process increases the interfacial area, and thus accelerates dimer production. At the same time, however, the presence of the dimers at the interface creates a "barrier" that hampers the diffusion and approach (to within the reaction distance r_0) of the to-be-reacted A and B particles. The net outcome of mixing is then determined by the interplay between these competing tendencies. Our results show that the extension of the interfacial area dominates and allows rapid and efficient mixing.

Of course, the details of these processes depend on the specific values of K and k. For example, for $K = 1$ and $k = 0.00001$, the wrinkled interface at $t \approx 10^6h$ had ~100 dimers (*vs.* 50 at the beginning of the simulation, *cf.* Fig. 1) while about 20 dimers were "immersed" into the non-reacted A and B liquids. The surfactant-like properties of the interfacial dimers lowered the effective surface tension. Then, wrinkling of the interface rapidly increased to the degree where some wrinkles separated from the interface and became micelles, some of them consisting of only dimers without "internal" A's or B's. Owing to slow reaction and low surface tension, however, the expanding surface was characterized by relatively low density of the dimers—consequently, it remained relatively permeable to unreacted A and B molecules. The kinetic plot in the leftmost graph in Fig. 2b shows that the production of dimers had a characteristic sigmoidal dependence indicating that the effect of rapidly increasing interfacial area outweighed any slow-down effects due to reduced interfacial permeability (of course, when the reaction substrates ran out, the production of dimers slowed down and the curve plateaued).

In contrast, for $K = 1$ and $k = 0.1$, the very fast reaction gave rise to a high dimer density at the interface even at an early times ~10^4h. Consequently, the interface effectively prevented the contact between the non-reacted A and B liquids, and the reaction became slow and driven by fluctuations only. At this time, the surface tension became small or even negative (see ref. 21), so the interface became unstable. The instability took the form of a cascade of break-ups of the non-reacted liquid regions into smaller and smaller vesicles of A and B particles. Each of these vesicles was encircled by a tight layer of dimers. At a certain size of the vesicles, the interfacial instability became ineffective and dimer production substantially slowed down but the system still consisted of relatively large aggregates of non-reacted particles encapsulated by dimers.

The $k = 0.001$ case was intermediate between the very slow and very fast reaction. At early times, the number of dimers rapidly increased but the density of interfacial dimers at the onset of interfacial instabilities and in the course of break-up cascade was smaller than for $k = 0.1$. Subsequently, the rapid increase of the interfacial area resulted in acceleration of dimer production, and an early completion of the reaction.[21] We note that for each value of the parameter K, there exists a different, optimal value of parameter k for which the reaction-completion time is minimal.

A remarkable feature of the collective mixing kinetics at large values of K was the aforementioned appearance of long filaments comprising dual layers of dimers and propagating into non-reacted liquids. Once a fluctuation created a small "finger" at the interface, the dimers at the base of the finger became proximal, forming a favorable back-to-back contacts (*i.e.*, AB···BA or BA···AB). These contacts stabilized the "finger" enough to let it grow or pinch off into a vesicle. As mentioned above, a dual layer is a filament of the laminar structure. For this configuration, the packing realizes the minimal local energy. This results in some rigidity of the dual-layer configuration. Locally, a dual-layer "finger" propagating into the A liquid had the B particles on the inside; for a dual layer in the B liquid, the inside part presented A particles. Another mechanism of creating dual-layer structures was by the droplets containing unreacted particles of either type to increase their aspect ratios (*i.e.*, becoming oblong) by overpopulating their surfaces with dimers while "loosing" the internal monomers. This mechanism led to either "flat" filaments or, if fluctuations prevailed, to the splitting of the large droplet into smaller "progenies". Interestingly, both types of processes were observed experimentally, albeit at larger, micrometre scales. For example, Weaver and co-workers[22] described a system in which interfacial protonation of amphiphilic branched copolymer surfactants (BCSs, based on methacrylic acid and poly(ethylene glycol)methacrylate with dodecane chain ends) evolved micron-sized droplets into spheroids and worm-like structures. Luisi's and Szostak's groups published a series of papers describing division of macroscopic droplets based on the interfacial reactions of surfactant molecules of various types.[14–16] The key message of our simulations is that similar phenomena could be observed at much smaller, molecular scales.

4. Conclusions

In summary, we studied a model 2D system in which a chemical reaction facilitates mixing at molecular scales. In this system, the

time-schedule of reaction (*i.e.*, of dimer production, Fig. 2b) and concomitant reactive mixing are determined by the competition between encapsulation (slowing down the reaction) and surface growth (accelerating the dimer production). The major role of the reaction is to destabilize the interface between the two liquids thus leading to various types of morphologies ranging from interfacial wrinkles, though "fingers," to vesicles and micelles. One interesting observation that merits further research is that for each set of controlling parameters there appears to exist an optimal value of the reaction rate parameter, k_{opt} (K,T,t), for which the number $N_d(t)$ of dimers at a given time t is maximized (see Fig. 2b). Most importantly, however, the concept of reactive mixing at molecular scales calls for experimental validation.

Acknowledgements

This work was supported by the Non-equilibrium Energy Research Center (NERC) which is an Energy Frontier Research Center funded by the US Department of Energy, Office of Science, Office of Basic Energy Sciences, under Award Number DE-SC0000989. A.P. thanks Drs M. Gelfer and V. Ginzburg (The Dow Chemical Company) for many fruitful discussions of reactions and mixing in polyurethanes.

Notes and references

1 W. Li, A. J. Ryan and I. K. Meier, Morphology development *via* reaction-induced phase separation in flexible polyurethane foam, *Macromolecules*, 2002, **35**, 5034–5032; 6306–6312.
2 M. J. Elwell, J. L. Stanford and A. J. Ryan, Structure Development in Reactive Systems, in *Processing of Polymers*, ed. H. E. H. Meijer, VCH Publishers, Weinheim, 1997, vol. 18.
3 V. V. Ginzburg, J. Bicerano, Ch. P. Christenson, A. K. Schrock and A. Z. Patashinski, Theoretical modeling of the relationship between Young's modulus and formulation variables for segmented polyurethanes, *J. Polym. Sci., Part B: Polym. Phys.*, 2007, **45**, 2123–2135.
4 A. Amini, G. De Cesare and A. Schleiss, Velocity profiles and interface instability in a two-phase fluid: investigations using ultrasonic velocity profiler, *Exp. Fluid.*, 2009, **46**, 683–692.
5 S. C. Machuga, H. L. Midje, J. S. Peanasky, Ch. W. Macosko and W. E. Ranz, Monodisperse interfacial mixing in fast polymerizations, *AIChE J.*, 1988, **34**, 1057–1064.
6 J. T. Davies and D. A. Haydon, *Spontaneous emulsification, 2nd International Congress of Surface Activity I*, 1957, pp. 417–418.
7 P. D. Wickert, C. W. Macosko and W. E. Ranz, Small-scale mixing phenomena during reaction injection-molding, *Polymer*, 1987, **28**, 1105–1110.
8 C. Almarcha, P. M. J. Trevelyan, P. Grosfils and A. De Wit, Chemically driven hydrodynamic instabilities, *Phys. Rev. Lett.*, 2010, **104**, 044501.
9 L. Rongy, P. M. J. Trevelyan and A. De Wit, Dynamics of A + B → C reaction fronts in the presence of buoyancy-driven convection, *Phys. Rev. Lett.*, 2008, **101**, 084503.
10 A. De Wit, P. De Kepper, K. Benyaich, G. Dewel and P. Borckmans, Hydrodynamical instability of spatially extended bistable chemical systems, *Chem. Eng. Sci.*, 2003, **58**, 4823–4831.
11 Y. Nagatsu and T. Ueda, Effects of reactant concentrations on reactive miscible viscous fingering, *AIChE J.*, 2001, **47**, 1711–1720.
12 J. E. Pearson, Complex pattern in a simple system, *Science*, 1993, **261**, 189–192.
13 K. Eckert, M. Acker and Y. Shi, Chemical pattern formation driven by a neutralization reaction. I. Mechanism and basic features, *Phys. Fluids*, 2004, **16**, 385–399.
14 P. A. Bachmann, P. Walde, P. L. Luisi and J. Lang, Self-replicating reverse micelles and chemical autopoiesis, *J. Am. Chem. Soc.*, 1990, **112**, 8200–8201.
15 P. A. Bachmann, P. Walde, P. L. Luisi and J. Lang, Self-replication micelles—aqueous micelles and enzymatically driven reactions in reverse micelles, *J. Am. Chem. Soc.*, 1991, **113**, 8204–8209.
16 T. F. Zhu and J. W. Szostak, Coupled growth and division of model protocell membranes, *J. Am. Chem. Soc.*, 2009, **131**, 5705–5713.
17 B. A. Grzybowski, *Chemistry in Motion. Reaction–Diffusion Systems for Micro- and Nanotechnology*, Wiley, Chichester, 2009.
18 A. C. Mitus, A. Z. Patashinski, A. Patrykiejew and S. Sokolowski, Local structure, fluctuations, and freezing in two dimensions, *Phys. Rev. B: Condens. Matter*, 2002, **66**, 184202.
19 The per-dimer change $\sim W(r_0)$ in the total energy makes dimer creation essentially irreversible because of the high binding strength imposed. Of course, at smaller values of parameter β and/or larger $|r - r_0|$, particles' unbinding becomes observable. In our algorithm, when the distance between some bound A and B increases beyond a preset threshold value, these particles are returned to the free-particle list. However, small unbinding probabilities do not affect reaction kinetics and simulation results perceptibly. For typical simulation parameters, $\beta = 150$, $\alpha = 100$, and $|r - r_0| < 0.02$, no unbinding events are observed at $T = 3$.
20 K. J. Strandburg, Two-dimensional melting, *Rev. Mod. Phys.*, 1988, **60**, 161–207.
21 One can assume two different regimes of the wrinkling. An equilibrium regime involves thermal fluctuations of the interface under conditions of decreased surface tension. Another much "faster" regime is non-equilibrium: due to fluctuations,reaction continues to add dimers onto the interface and creates overpopulation (a compressed dimer system) of dimers therein. This compression and the attraction of dimers to the interface make the surface tension effectively negative. We suggest that the rapidly developing interface instabilities observed in our simulations at fast reaction rates, especially in the form of fingering, are manifestation of negative surface tension σ. A qualitative explanation of the observed fingering is then as follows: unlike in the case of positive surface tension, the direction of the Laplace pressure $\Delta P = \sigma/R$ for a negative surface tension is from the center of curvature outwards. This pressure is then acting to increase the curvature and create fingers propagating into non-reacted liquids. The velocity of fingers' propagation is determined by the viscosity of the liquids because the motion of the interface involves hydrodynamic motion in the surrounding liquid. As seen in the simulations, propagating finger-like structures brake-up larger regions of non-reacted particles into smaller and smaller drops decorated by dimers.
22 J. V. M. Weaver, S. P. Rannard and A. I. Cooper, Polymer-mediated hierarchical and reversible emulsion droplet assembly, *Angew. Chem., Int. Ed.*, 2009, **48**, 2131–2134.